A Study of the Three-Dimensional Particle Size Segregation Structure in a Rotating Drum

A. N. Huang and H. P. Kuo

Dept. of Chemical and Materials Engineering, Chang Gung University, Tao-Yuan 333, Taiwan

Three-dimensional particle size segregation structures of binary mixtures of six different size ratios (SR = 1.42–3.37) in a rotating drum are studied. The formation of two smaller particle satellites around the central smaller-particle rich band after the band formation core-thickening mechanism is reported for the first time. The binary mixtures of six SRs show three satellite shapes, including the small bump shape, the axe shape, and the hemisphere shape. Except for the binary mixture of SR = 2.01 with the axe satellite shape, the satellite size increases with the increasing of the SR value at the same bed depth. The degrees of mixing of binary mixtures of six different SRs at different bed depths are analyzed using the Lacey mixing index. The degree of mixing at the bed surface and close to the drum cylindrical wall can be explained by the drift-diffusional model of Savage (1993). © 2011 American Institute of Chemical Engineers *AIChE J*, 58: 1076–1083, 2012

Keywords: mixing, solids processing, particle technology, particulate flows

Introduction

Rotating drums are commonly used for mixing, drying, and granulation operations of solids in chemical, pharmaceutical, and food industries. As the granular particles in a rotating drum perform rich physical behaviors, extensive research work has been carried out to study the flow regimes,[1] the solids mixing/segregation behaviors,[2–4] and the heat transfer behaviors in rotating drums.[5] Most of these work addressed the problems at the surface of the bed from the end views[6,7] or from the top views.[8,9] The information inside the bed was less discussed. The magnetic resonance imaging techniques,[10,11] the positron emission particle tracking techniques,[12–14] and the computational simulations[15–17] are few methods, which can obtain the information inside the bed.

There are several reasons causing the granular mixture to mix or to segregate in a rotating drum. When particles with different particle sizes, shapes, densities, roughness, or elasticity are mixed in a drum, they tend to segregate.[18,19] When

a binary granular mixture of different sizes is tumbled in a rotating drum, smaller particles are concentrated in the bed center and larger particles are accumulated close to the bed periphery after several revolutions due to the percolation mechanism, forming a segregation core. Following the formation of the segregation core, alternative larger-particle and smaller-particle rich bands are observed at the bed surface.[19] Khan et al.[20] suggested that the formation of the bands was due to the core-thickening mechanism of smaller particle. As the formation of the bands always begins next to the two end walls, Kuo et al.[21] argue that the end wall shearing plays a role in the formation of the bands. Zik et al.[22] studied segregation in three different rotating tubes with the same mean diameter but with different shapes: cylindrical, periodic radial modulation, and screw-like modulation. In some experimental conditions, while no segregation occurred in the cylindrical tube, the tube with periodic radial modulations locked bands in space and induced segregation. They inferred that segregation resulted from instability analogous to spinodal decomposition.

Depending on the fill levels and the rotational speeds of the drum, granular flows in a rotating drum show six flow regimes.[1] The rolling regime is probably the most frequently

Correspondence concerning this article should be addressed to H. P. Kuo at hpkuo@mail.cgu.edu.tw.
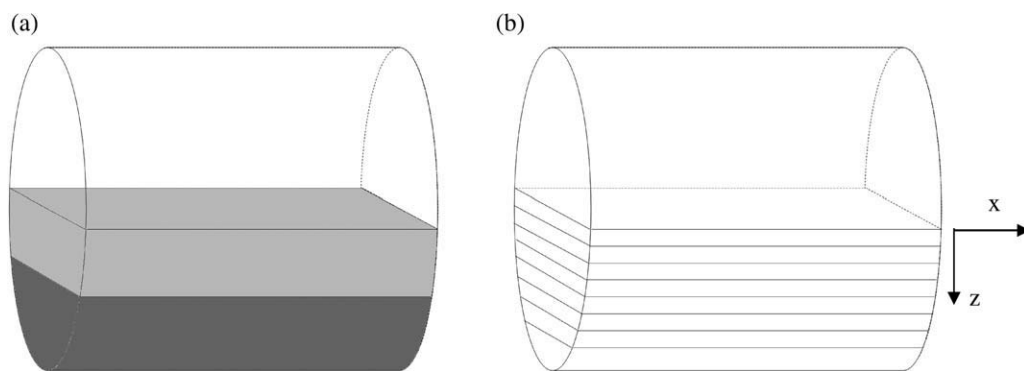
Figure 1. (a) The initial condition: the smaller particles (light gray) were horizontally loaded on top of the larger particles (dark gray); (b) the segregation patterns were observed at z = 0 (bed surface), 0.5, 1, 1.5, 2, 2.5, 3, 3.5, and 4 cm.

operated flow regime in industry. In this article, we also study solids segregation in a drum operated in the rolling mode. In the rolling regime, the particle bed shows a passive zone and an active zone, where little or no mixing occurs in the passive zone.[23] The particles in the active zone roll down the bed-free surface and mixing occurs. The thickness of the active zone increases with the increasing of the drum-to-particle size ratio.[24]

In this study, binary glass bead mixtures of six different size ratios, SRs were tumbled in a horizontally rotating drum. The internal structure of the drum was investigated and the three-dimensional (3-D) segregation structure was constructed for the first time. The degrees of mixing at different bed depths were also analyzed and discussed.

Experimental Method

The segregation studies were performed in a partially filled drum horizontally placed on a pair of rollers, in a similar way to a ball mill. The drum was 98 mm in diameter and 100 mm in length. The cylindrical column of the drum was made of stainless steel and the two end walls were made of glass to ease the end-view observation. The cylindrical column of the drum was cut into two shells through the plane along the rotational axis. The two half tubes could be joined together by two outer rings. The drum has been used to study high fill level drum segregation patterns.[25] The rotational speed of the drum was set at 11.4 rpm and the granular flow was in the rolling mode.

Binary glass beads (density ∼2521 kg m^{-3}) of six different SRs were mixed in the rotating drum. The larger particle of the binary mixture was 0.71–0.84 mm and dyed black. The smaller particle of the binary mixtures was white and was 0.59–0.50 mm, 0.50–0.42 mm, 0.42–0.35 mm, 0.35–0.297 mm, 0.297–0.25 mm, or 0.25–0.21 mm. Hence, the SR of the binary mixtures was 1.42, 1.68, 2.01, 2.40, 2.83, or 3.37. The glass beads were dried in a 100°C oven for 30 min before each experimental run. The dynamic angle of repose of the glass beads was measured using the same drum rotating at 11.4 rpm and 50% fill level. It is difficult to determine the dynamic angle of repose unambiguously, because the bed surface is not always flat (especially the smallest particles) and the dynamic angles of repose immediately next to the end walls and far from the end walls may be different.[26] Here, the dynamic angle of repose of the particles immediately next to the end walls was measured by the photos taken from the end-view CCD camera.

In a typical run, an equal-apparent volume mixture of smaller and larger beads was filled in the drum with a total fill level of 50%. The smaller particles placed on top of the larger particles was set as the initial condition (Figure 1a). The humidity of the environment was carefully controlled at 60–62%.

After the experimental run, 96°C agar solution (1 wt%) was gently poured onto the bed without damaging the bed structure. The granular bed was "frozen" after the gelation of the agar solution.[25] The bed was sliced in the z-direction by a knife, and the segregation patterns on the plane along the rotational axis at the bed depths 0 (free surface), 0.5, 1, 1.5, 2, 2.5, 3, 3.5, and 4 cm were recorded by a CCD camera (Figure 1b). One particular experiment was carried out using the binary mixture of SR = 1.42 mixing for 90 min, the segregation patterns did not show noticeable differences when comparing to those obtained from the 15-min experiment. The segregation structure after 15 min rotation was considered reaching its steady state and every experimental run was set as 15 min in this study.

The degree of mixing at different bed depths was quantified using the Lacey mixing index (MI).[27] The Lacey MI uses the key component composition variance to calculate the degree of mixing. As the black pixel concentration in a cell is analogy to the composition of the key component in the withdrawn sample, the black pixel concentration in the segregation pattern photo was used to replace the key component composition in the Lacey MI calculations. The size of the cell should be large enough to reach the scale of scrutiny and be small enough to reveal the local degree of mixing information. We tested several cell sizes, and the cell size of 0.33 cm × 0.33 cm (approximately the size of 19 black particles) was found to be the most appropriate cell size.

The photo taken at the corresponding bed depth was divided into 0.33 cm × 0.33 cm cells. The concentrations of the black pixels in all the cells were calculated, and the degree of mixing at a given bed depth was calculated by the Lacey MI as,

$$\text{MI} = \frac{\sigma_0^2 - \sigma^2}{\sigma_0^2 - \sigma_R^2} \qquad (1)$$
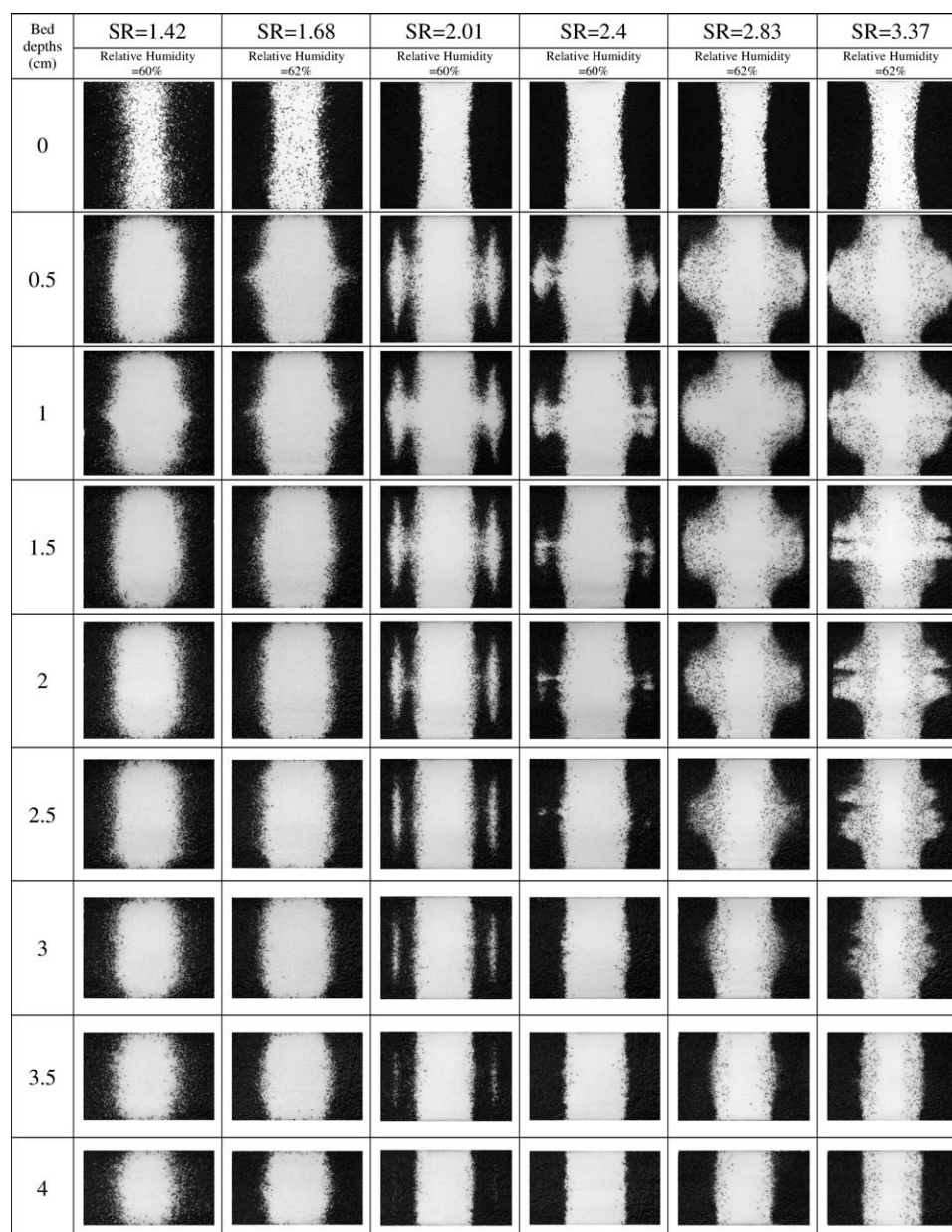
Bed depths (cm)	SR=1.42 Relative Humidity =60%	SR=1.68 Relative Humidity =62%	SR=2.01 Relative Humidity =60%	SR=2.4 Relative Humidity =60%	SR=2.83 Relative Humidity =62%	SR=3.37 Relative Humidity =62%
0						
0.5						
1						
1.5						
2						
2.5						
3						
3.5						
4						

Figure 2. The segregation patterns obtained at different depths of the bed (0, 0.5, 1, 1.5, 2, 2.5, 3, 3.5, and 4 cm below the surface) for binary mixtures of different SR values.

where σ_0^2 is the variance of the black pixel concentrations of all the cells at a given bed depth while the binary mixture was completely segregated; σ_R^2 is the variance of the black pixel concentrations of all the cells at a given bed depth while the binary mixture was fully randomly mixed; σ is the variance of the black pixel concentrations of all the cells from the photo taken at a given bed depth. When the concentrations of the black pixel in all the cells are 50%, MI = 1, and the mixture is perfectly mixed.
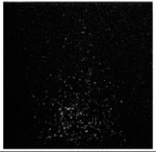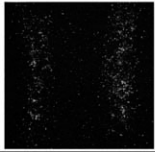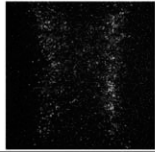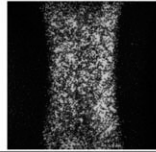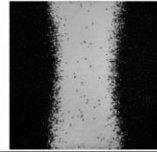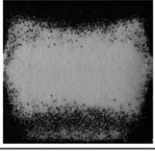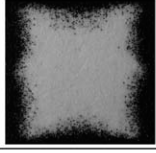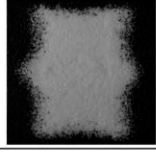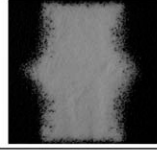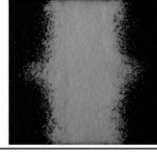
Results and Discussion

Figure 2 shows the segregation patterns at different depths of the bed. At the surface of the bed, the interface between the black larger-particle rich band and the white smaller-

particle rich band becomes more distinguishable when SR increases from 1.42 to 2.01. When SR increases from 2.01 to 3.37, although the number of larger particles on the surface of the smaller-particle rich band increases, the interface between the larger-particle rich band and the smaller-particle rich band is still clearly observed.

The existence of the smaller particle core (i.e., the two white satellites around the central white band) appears from 0.5 cm below the bed surface for all particle SRs, except for SR = 1.42. There is no core when SR = 1.42, and this value is quite close to the reported threshold value for size-induced segregation to occur.[28] If a core exists, the size of the core decreases with the increasing of the bed depth. The satellite shapes are different for binary mixtures of different SR values. When SR is small (say 1.68), the satellite is small.

(a) SR=1.68

Bed depths (cm)	0.5min T=18.6℃, H=62%	1.5min T=19.3℃, H=60%	3min T=20.1℃, H=55%	6min T=20.5℃, H=56%	15min T=19.8℃, H=60%
0					
1					
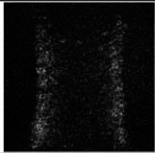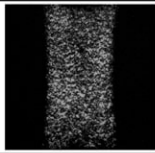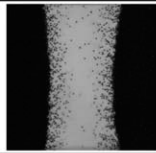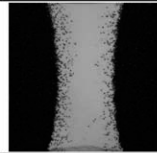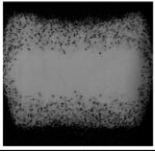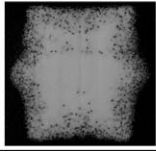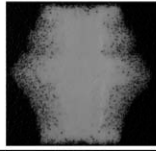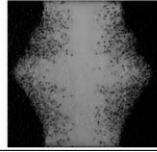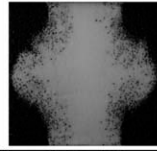
(b) SR=3.37

Bed depths (cm)	0.5min T=19.3℃, H=60%	1.5min T=19.9℃, H=62%	3min T=20.5℃, H=57%	6min T=20.6℃, H=60%	15min T=18.9℃, H=61%
0					
1					

Figure 3. The formation of the segregation structure of binary mixture of (a) SR = 1.68 (tortuous); (b) SR = 3.37.

There is only a small bump next to the white segregation band. A satellite-free band segregation structure may be obtained for the binary mixture with small SR values. When SR = 2.01, the shape of the satellite is similar to an axe with its sharp edge facing down into the bed and may disconnect to the white segregation band while further down into the bed. When SR is large (say 2.83 and 3.37), the satellite is a hemisphere attached to the white segregation band. When SR = 2.4 (i.e., between 2.01 and 2.83), the shape of the satellite is a combination of an axe shape and a hemisphere shape. Except for SR = 2.01 with the unusual satellite axe shape, the size of the satellite increases with the increasing SR value at the same bed depth. This is of expectation because the core formation percolation mechanism is enhanced with the increasing of the SR value.

The formation of the two satellites around the central band is reported for the first time. In previous reports, the formation of the segregated core comes earlier than the formation of the segregated bands. Because of the so-called core-thickening mechanism,[20] the smaller particles within the core migrate to the center of the drum from the two ends, causing the formation of a smaller-particle rich band at the center of the drum. However, the results in Figure 2 indicate that the core particles do not entirely migrate to the central smaller-particle rich band and the residuals form two intriguing satellites around the central band. Figure 3 shows the formations of the two type satellites at the surface and at 1 cm below the bed. The snapshots were taken from the top

view after 0.5, 1.5, 3, 6, and 15 min rotational time. When the rotational time increases, the concentration of the smaller particles at the drum center was increased, and the larger particles were expelled toward the two ends. The final segregation structures of the binary mixtures of different SRs were obtained after 15-min experimental time. The migration of the smaller particles by the core-thickening mechanism is further discussed.

The core-thickening mechanism is caused by the diffusional migration of the smaller particles from the two ends to the drum center. Savage (1993) proposed the relation for the particle axial diffusion coefficient based on hard-particle dynamics simulation and the diffusion coefficient is proportional to the solids voidage.[29,30] As the larger particles are of the same size in all the experimental runs, the solids voidage is smaller with greater SR values (i.e., the particles are more densely packed), causing a smaller particle diffusional coefficient value. The suppressed smaller particle diffusion causes the larger particles being expelled to a less extent. Thus, it is the SR value determines the speed of the migration of the smaller particles, causing the formation of the satellites of different shapes.

As the segregation patterns at different bed depths have been obtained, the 3-D segregated structures of binary mixtures of six SRs were constructed and shown in Figure 4. In Figure 4, the concentrations of the "white" pixels in 0.33 cm × 0.33 cm cells in photos in Figure 2 were calculated and shown as the "gray" scale concentration contour plots in
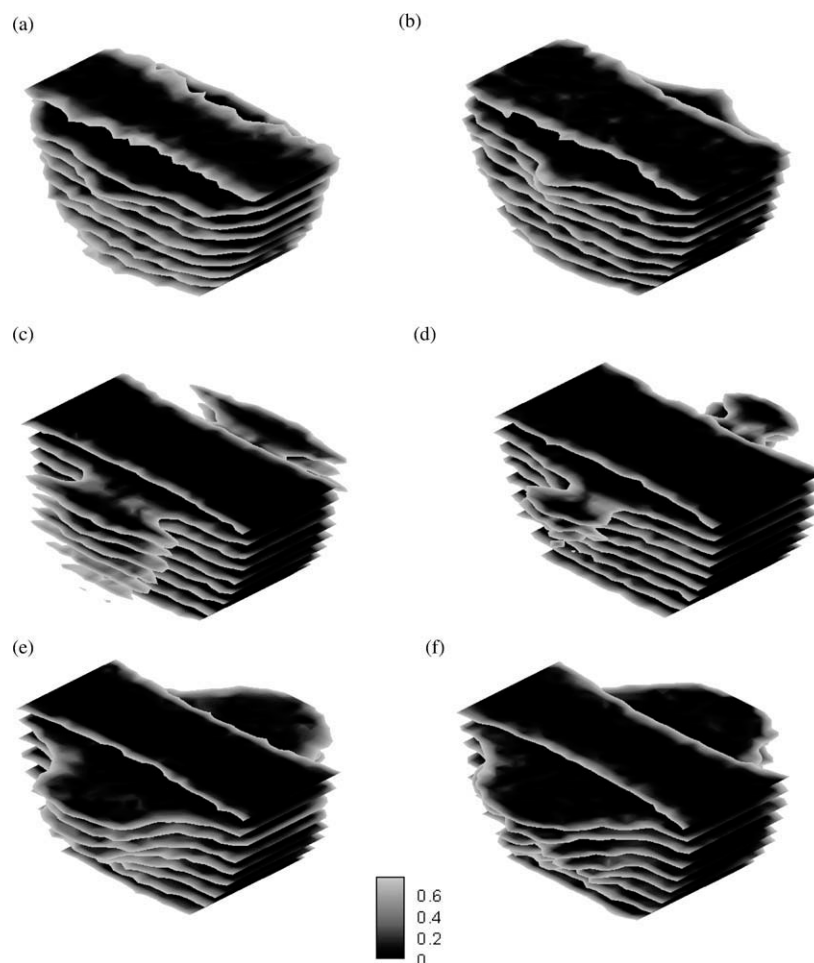
Figure 4. The three-dimensional segregated structure of the smaller particles of binary mixtures of the size ratio: (a) SR = 1.42; (b) SR = 1.68; (c) SR = 2.01; (d) SR = 2.40; (e) SR = 2.83; (f) SR = 3.37. The gray scale represents the black pixel concentration in a given cells. "0" means 100% smaller particles and "1" means 100% larger particles.

Figure 4 to ease the segregation structure investigation. As far as the authors' knowledge, the "direct" construction of the 3-D drum segregation structure is reported for the first time. Researchers argue that the particles of similar properties tend to gather and cause segregation. As the particles of the binary mixtures are differing only in sizes, the results in Figure 4 indicate that the size and shape of the segregated structure are not the simple functions of the particle SR. The mechanisms of the size-induced particle segregation are complicated and may not be simply realized by the percolation mechanism.

The Lacey MI was used to quantify the degree of mixing at different bed depths, and the results are shown in Figure 5. Figure 5a shows that the values of the MI changes more dramatically at the surface of the bed (i.e., 0 cm) and close to the drum cylindrical wall (i.e., 4 cm) when comparing with the changes of the MI values at other bed depths for most SRs. Therefore, we show the relationships between the degree of mixing and the SR in Figures 5b,c by two groups: (1) at the surface of the bed and close to the drum cylindrical wall and (2) at the rest of the bed depths, respectively. In Figure 5b, the MI

value decreases with the increasing of SR from 1.42 to 2.40 and slightly increases when SR increases from 2.83 to 3.37. In Figure 5c, the MI values fluctuate as the SR increases. Although the result in Figure 5c lacks plausible explanations, the result in Figure 5b (i.e., the bed free surface and the immediate rolled down layer hid at the deepest of the bed) can be explained by a drift-diffusional model.[29,30]

The total flux current of particle motion at the bed surface consists a drift current (J_{drift}) and a diffusional current (J_{diff}),

$$J_{total} = J_{drift} + J_{diff} \qquad (2)$$

with

$$J_{drift} = -\beta \frac{\partial z}{\partial x} \qquad (3)$$

and

$$J_{diff} = -D \frac{\partial C(x,t)}{\partial x} \qquad (4)$$

where β is the drift coefficient and is a monotonic function of the difference of dynamic angle of repose between the large
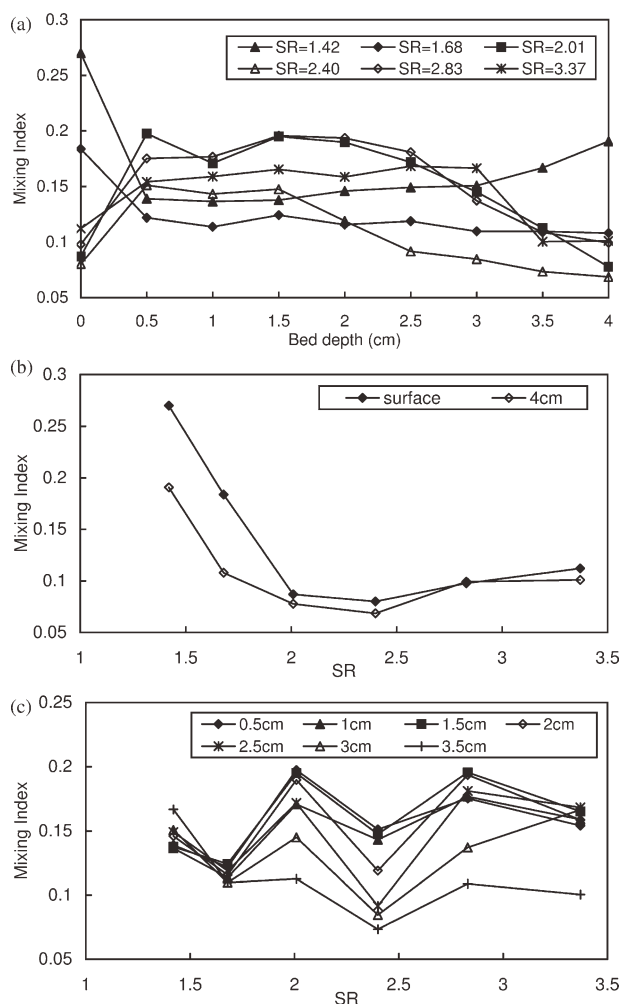
Figure 5. The Lacey Mixing Index analysis of the segregation patterns in Figure 2.

(**a**) at different bed depths for binary mixtures of different SR values; (**b**) at bed surface and 4 cm below the bed surface; (**c**) 0.5, 1, 1.5, 2, 2.5, 3, and 3.5 cm below the bed surface.

particle and the small particle; $-\frac{\partial z}{\partial x}$ is the transverse slope (see Figure 1 for the coordination); D is the axial diffusion coefficient; $C(x,t)$ is the concentration of the key component (i.e., the black larger particles) at position x at rotational time t.

The dynamic angles of repose of the particles are shown in Figure 6a, and the differences of the angles of repose of binary mixtures of different SRs are shown in Figure 6b. When the SRs of binary mixture increase from 2.40 to 3.37, the differences of the angles of repose increase first but decrease subsequently. As the drift coefficient and is a monotonic function of the difference of dynamic angle of repose between the large particle and the small particle, the result in Figure 6b indicates that the MI profile in Figure 5b cannot be explained by the particle drift coefficient only. The transverse slope in Eq. 3 should be considered. The transverse slope is closely related to the shape of the free surface.

We observed two different binary mixture free surface shapes from all the experimental runs. The schematic diagrams of the free surfaces of binary mixture of smaller SR

(SR = 1.42–2.40) and larger SR (SR = 2.83–3.37) are shown in Figures 7a and b, respectively. The top and bottom of the free surfaces of the larger-particle rich band and the smaller-particle rich band are of the same vertical position for the binary mixture of SR = 1.42–2.40 and the differences of the angles of repose of the binary mixture are statistically zero (Figure 6a). The only difference is the slightly concave free surface of the smaller-particle rich band. Because there is no difference of the angles of repose between the larger and the smaller particles, the drift current may be neglected and the diffusional current dominates. When the particle SR increases, the diffusional coefficient decreases (see earlier). The dominating mixing diffusional current is suppressed with the increasing of the SR value, causing MI decreases when SR increases from 1.42 to 2.40 in Figure 5b.

In Figure 7b, the positions 1/3 from the bottoms of the free surfaces of the larger-particle rich band and the smaller-particle rich band are about the same vertical position. The particles at the larger-particle rich band are easily to roll down to the surface of the smaller-particle rich band at the upper part of the band interface and roll down from the smaller-particle rich band to the larger-particle rich band at the lower part of the band interface. The drift currents are shown in Figure 7b using four coarse arrows. The particles also move from the relatively high-concentration band to the relatively low concentration band by the diffusion mechanism, and the diffusional currents are shown in Figure 7b using two fine arrows.
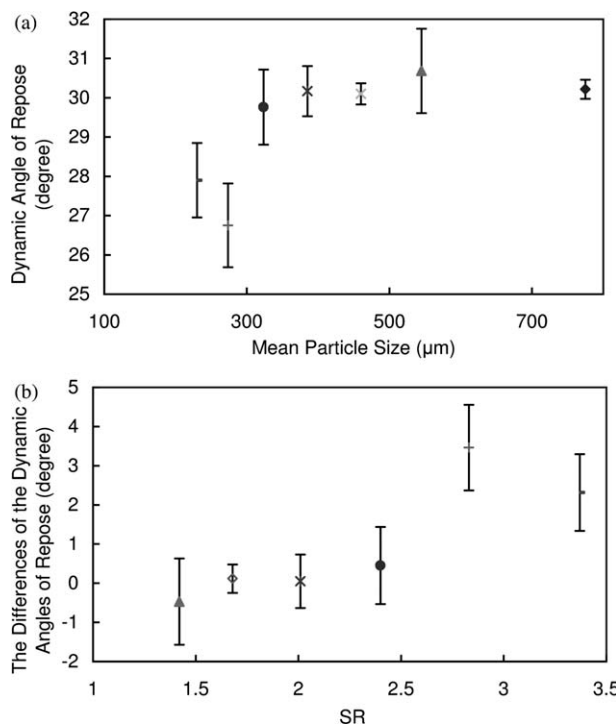

Figure 6. (a) The measured dynamic angles of repose of particles of different sizes (5 times measurements). (b) The differences of the dynamic angles of repose of binary mixtures of different size ratios.
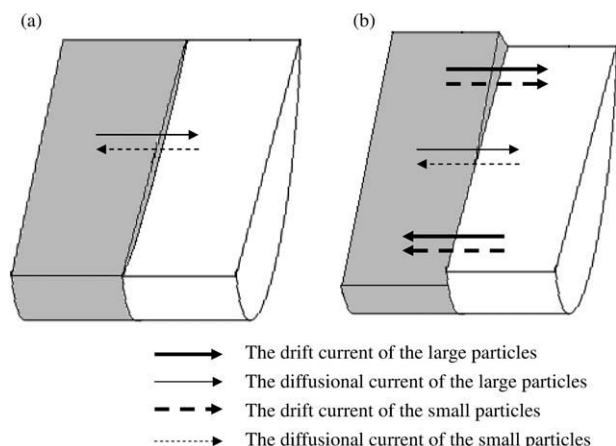
Figure 7. Schematic diagrams of the free surfaces of binary mixture of (a) smaller size ratio, SR = 1.42–2.40, and (b) larger size ratio, SR = 2.83–3.37.

The drift and diffusional currents of the larger particles and the smaller particles are also schematically presented. The larger-particle rich band is gray and the smaller-particle rich band is white.

The differences of the angles of repose of the binary mixture of SR = 2.83–3.37 are between 1.34° and 4.56° in Figure 6b. As the drift coefficient is not zero, the transverse slope in Equation (3) should be considered in the drift current estimation. Although the drift coefficient decreases and the diffusional current decreases when SR increases from 2.83 to 3.37, the transverse slope $-\frac{\partial z}{\partial x}$ increases when SR increases from 2.83 to 3.37 from our visual observation. The increasing of the transverse slope compensates the decreasing of the drift coefficient and the diffusional current, causing MI increases when SR increases from 2.40 to 3.37 in Figure 5b.

Conclusions

Segregation of binary glass beads of six in a horizontally rotating drum was studied. The 3-D segregation structure was constructed using gel-slicing and imaging-editing methods. The residuals of the core after the band formation core-thickening mechanism produced two satellites around the central smaller-particle rich band. Binary mixtures of different SRs show satellites of different shapes, including the small bumps next to the central band shape, the axe shape, and the hemisphere shape. Except for the binary mixtures of SR = 2.01 with the unusual axe satellite shape, the size of the satellite increases with the increasing of the SR value at the same bed depth.

The Lacey MI analysis shows that the degree of mixing of the bed includes two groups: (1) at the surface of the bed and close to the cylindrical wall and (2) at the rest of the bed depths. The relationship between the particle SR and the degree of mixing at the surface of the bed and close to the drum cylindrical wall can be explained by the drift-diffusional model of Savage (1993).

Acknowledgments

Literature Cited

1. Henein H, Brimacombe JK, Watkinson AP. Experimental study of transverse bed motion in rotary kilns. *Metall Mater Trans B*. 1983; 14:191–205.
2. Khakhar DV, McCarthy JJ, Shinbrot T, Ottino JM. Transverse flow and mixing of granular materials in a rotating cylinder. *Phys Fluids*. 1997;9:31–43.
3. Dury CM, Ristow GH. Competition of mixing and segregation in rotating cylinders. *Phys Fluids*. 1999;11:1387–1394.
4. Metcalfe G, Graham L, Zhou J, Liffman K. Measurement of particle motions within tumbling granular flows. *Chaos*. 1999;9:581–593.
5. Stroem LK, Desai DK, Hoadley AFA. Superheated steam drying of Brewer's spent grain in a rotary drum. *Adv Powder Technol*. 2009; 20:240–244.
6. Khakhar DV, Orpe AV, Ottino JM. Continuum model of mixing and size segregation in a rotating cylinder: concentration-flow coupling and streak formation. *Powder Technol*. 2001;116:232–245.
7. Hill KM, Gioia G, Amaravadi D, Winter C. Moon patterns, sun patterns, and wave breaking in rotating granular mixtures. *Complexity*. 2005;10:79–86.
8. Choo K, Baker MW, Molteno TCA, Morris SW. Dynamics of granular segregation patterns in a long drum mixer. *Phys Rev E*. 1998; 58:6115–6123.
9. Charles CRJ, Khan ZS, Morris SW. Pattern scaling in axial segregation. *Granul Matter*. 2006;8:1–3.
10. Nakagawa M, Altobelli SA, Caprihan A, Fukushima E. NMRI study: axial migration of radially segregated core of granular mixtures in a horizontal rotating cylinder. *Chem Eng Sci*. 1997;52:4423–4428.
11. Kawaguchi T. MRI measurement of granular flows and fluid-particle flows. *Adv Powder Technol*. 2010;21:235–241.
12. Ding YL, Seville JPK, Forster R, Parker DJ. Solids motion in rolling mode rotating drums operated at low to medium rotational speeds. *Chem Eng Sci*. 2001;56:1769–1780.
13. Ingram A, Seville JPK, Parker DJ, Fan X, Forster RG. Axial and radial dispersion in rolling mode rotating drums. *Powder Technol*. 2005;158:76–91.
14. Kuo HP, Knight PC, Parker DJ, Seville JPK. Solids circulation and axial dispersion of cohesionless particles in a V-Mixer. *Powder Technol*. 2005a;152:133–140.
15. Rapaport DC. Radial and axial segregation of granular matter in a rotating cylinder: a simulation study. *Phys Rev E*. 2007;75:art no. 031301.
16. Arntz MMHD, Den Otter WK, Briels WJ, Bussmann PJT, Beeltink HH, Boom RM. Granular mixing and segregation in a horizontal rotating drum: a simulation study on the impact of rotational speed and fill level. *AIChE J*. 2008;54:3133–3146.
17. Iwasaki T, Yabuuchi T, Nakagawa H, Watano S. Scale-up methodology for tumbling ball mill based on impact energy of grinding balls using discrete element analysis. *Adv Powder Technol*. 2010;21: 623–629.
18. Williams JC, Khan MI. The mixing and segregation of particulate solids of different particle size. *Chem Eng*. 1973;269:19–25.
19. Kuo HP, Hsiao YC, Shih PY. A study of the axial segregation in a rotating drum using deformable particles. *Powder Technol*. 2006a; 166:161–166.
20. Khan ZS, Tokaruk WA, Morris SW. Oscillatory granular segregation in a long drum mixer. *Europhys Lett*. 2004;66:212–218.
21. Kuo HP, Hsu RC, Hsiao YC. Investigation of axial segregation in a rotating drum. *Powder Technol*. 2005b;153:196–203.
22. Zik O, Levine D, Lipson SG, Shtrikman S, Stavans J. Rotationally induced segregation of granular materials. *Phys Rev Lett*. 1994;73: 644–647.
23. Boateng AA, Barr PV. Modelling of particle mixing and segregation in the transverse plane of a rotary kiln. *Chem Eng Sci*. 1996;51:4167–4181.
24. Félix G, Falk V, D'Ortona U. Segregation of dry granular material in rotating drum: experimental study of the flowing zone thickness. *Powder Technol*. 2002;128:314–319.
25. Kuo HP, Shih PY, Hsu RC. Coupled axial-radial segregation in rotating drums with high fill levels. *AIChE J*. 2006b;52:2422–2427.
26. Dury CM, Ristow GH, Moss JL, Nakagawa M. Boundary effects on the angle of repose in rotating cylinders. *Phys Rev E*. 1998;57: 4491–4497.
27. Lacey PMC. Developments in the theory of particle mixing. *J Appl Chem*. 1954;4:257–268.

28. Williams JC. The mixing of dry powders. *Powder Technol*. 1968;2: 13–20.
29. Savage SB. Chapter 9: disorder, diffusion and structure formation in granular flows. In: Bideau D, Hansen A, editors. *Disorder and Granular Media*. North-Holland, Amsterdam, 1993:255–285.
30. Ottino JM, Khakhar DV. Mixing and segregation of granular materials. *Annu Rev Fluid Mech*. 2000;32:55–91.
31. Hill KM, Kakalios J. Reversible axial segregation of rotating granular media. *Phys Rev E*. 1995;52:4393–4400.
32. Choo K, Molteno TCA, Morris SW. Traveling granular segregation patterns in a long drum mixer. *Phys Rev Lett*. 1997;79: 2975–2978.